Inorg. Chem. **2006**, *45*, 5008–5017

Preparation, Properties, and Reactivities of Unprecedented Oxo-Sulfido Nb(IV) Aqua Ions and Crystal Structure of $(Me_2NH_2)_6[Nb_5(\mu_3\text{-}S)_2(\mu_3\text{-}O)_2(\mu_2\text{-}O)_2(NCS)_{14}]\cdot 3.5H_2O$

Bee-Lean Ooi,*,† Inger Søtofte,† Maxim N. Sokolov,‡ Svetlana G. Kozlova,‡,§ Søren B. Rasmussen,† Loa C. Nielsen,† and Jonas Henriksen†

Department of Chemistry, Technical University of Denmark, Kemitorvet, Building 207, Kongens Lyngby, Denmark, Nikolaev Institute of Inorganic Chemistry, Russian Academy of Sciences, Prospekt Lavrentyeva 3, Novosibirsk 630090, and Boreskov Institute of Catalysis, Russian Academy of Sciences, Prospekt Akademika Lavrentyeva 5, Novosibirsk 630090, Russia

Received December 16, 2005

By treatment of Zn-reduced ethanolic solutions of $NbCl_5$ with HCl in the presence of sulfide followed by cation-exchange chromatography, two oxo-sulfido niobium aqua ions, the red $[Nb_4(\mu_4\text{-}S)(\mu_2\text{-}O)_5(H_2O)_{10}]^{4+}$ and the yellow-brown $[Nb_5(\mu_3\text{-}S)_2(\mu_3\text{-}O)_2(\mu_2\text{-}O)_2(H_2O)_{14}]^{8+}$, were isolated. Both readily form their respective thiocyanate complexes, for which the structure for the former has been previously reported. Brown crystals of $(Me_2NH_2)_6[Nb_5S_2O_4(NCS)_{14}]\cdot 3.5H_2O$ (**1**) were isolated in the case of the latter, and the structure was determined by X-ray crystallography (space group: $a = 15.4018(5)$ Å, $b = 21.1932(8)$ Å, $c = 22.0487(8)$ Å, $\alpha = \gamma = 90°$, $\beta = 103.4590(10)°$, and $R_1 = 0.0659$). An unprecedented pentanuclear $Nb_5S_2O_4^{8+}$ core is revealed in which short Nb–Nb distances (2.7995(8)–2.9111(8) Å) are consistent with metal–metal bonding. A stopped-flow kinetic study of the 1:1 equilibration of NCS^- with $[Nb_4(\mu_4\text{-}S)(\mu_2\text{-}O)_5(H_2O)_{10}]^{4+}$ has been carried out. Equilibration rate constants are independent of $[H^+]$ in the range investigated (0.5–2.0 M) and at 25 °C; $k_f = 9.5\ M^{-1}\ s^{-1}$, $k_{aq} = 2.6 \times 10^{-2}\ s^{-1}$, and $K = 365\ M^{-1}$. Conditions with first NCS^- and then $[Nb_4(\mu_4\text{-}S)(\mu_2\text{-}O)_5(H_2O)_{10}]^{4+}$ in excess revealed a statistical factor of 4, suggesting the presence of four kinetically equivalent Nb atoms. Attempts to study the 1:1 substitution of NCS^- with $[Nb_5(\mu_3\text{-}S)_2(\mu_3\text{-}O)_2(\mu_2\text{-}O)_2(H_2O)_{14}]^{8+}$ showed signs of saturation kinetics. Quantum chemical calculations using the density functional theory (DFT) approach were performed on both the $Nb_4O_5S^{4+}$ and $Nb_5O_4S_2^{8+}$ naked clusters. The highest occupied and lowest unoccupied molecular orbitals have dominant Nb(4d) character. The HOMO for $Nb_4O_5S^{4+}$ is a nondegenerate fully filled MO, whereas for $Nb_5O_4S_2^{8+}$, it is a nondegenerate partially filled MO with one unpaired electron. EPR spectroscopy on $[Nb_5(\mu_3\text{-}S)_2(\mu_3\text{-}O)_2(\mu_2\text{-}O)_2(H_2O)_{14}]^{8+}$ shows that the molecule has total anisotropy (C_{2v}), with all three tensors, $\mathbf{g}_x = 2.399$, $\mathbf{g}_y = 1.975$, and $\mathbf{g}_z = 1.531$, resolved. No hyperfine interaction expected from the nuclear moment of $I = 9/2$ for ^{93}Nb was observed.

Introduction

There has been intense activity in the study of the aqueous solution chemistry of molybdenum and tungsten, where cuboidal $[M_4S_4]^{n+}$ and incomplete cuboidal $[M_3S_4]^{n+}$ units have emerged as important entities.[1] A series of mixed oxo-sulfido species, $[M_3O_{4-x}S_x(H_2O)_9]^{4+}$, as well as the selenium analogues have been extensively investigated and their syntheses well-defined.[1,2]

The aqueous solution chemistry of niobium, on the other hand, remains largely unexplored. Since the report on the first aqua ion of niobium, purportedly the green $[Nb_3O_4(H_2O)_9]^{3+}$ ion (later evidence favors the formulation of $[Nb_3(Cl)O_3(H_2O)_9]^{4+}$), which was crystallized as thiocyanate derivative $(NH_4)_3(Me_4N)_3[Nb_3SO_3(NCS)_9]\cdot MeOH$ in 1986,[3,4]

* To whom correspondence should be addressed. E-mail: obl@kemi.dtu.dk.
† Technical University of Denmark.
‡ Nikolaev Institute of Inorganic Chemistry, Russian Academy of Sciences.
§ Boreskov Institute of Catalysis, Russian Academy of Sciences.

(1) Hernandez-Molina, R.; Sykes, A. G. *J. Chem. Soc., Dalton Trans.* **1999**, 3137.
(2) Sakane, G.; Shibahara, T. *Inorg. Synth.* **2002**, *33*, 144−149. Fedin, V. P.; Sykes, A. G. *Inorg. Synth.* **2002**, *33*, 162−170.
(3) Cotton, F. A.; Diebold, M. P.; Llusar, R.; Roth, W. J. *J. Chem. Soc., Chem. Commun.* **1986**, 1276.

10.1021/ic052145i CCC: $33.50
Published on Web 05/25/2006

the dimeric $[Nb_2(\mu_2\text{-}S_2)_2(H_2O)_8]^{4+}$ aqua ion is the only other aqua complex of niobium reported.[5] Very different synthetic approaches were employed, with the trimeric complex being synthesized by treatment of $[Nb_2Cl_6(tht)_3]$ (tht = tetrahydrothiophene) with concentrated hydrochloric acid, whereas the dimeric complex was obtained from the polymeric NbS_2Cl_2 lead-in compound by reaction with potassium thiocyanate followed by treatment of the melt with water. [5]

We have recently described a convenient and versatile synthetic route to lower oxidation states of niobium.[6] Easy access to niobium complexes in aqueous solutions was achieved through the reduction of $NbCl_5$ in ethanol with zinc followed by treatment with aqueous acids. This opens up exciting possibilities into oxo-sulfido niobium cluster chemistry in aqueous solution. Indeed, when the reaction was carried out in the presence of a sulfide source, two new sulfide-containing aqua ions, a red and a yellow-brown, were obtained. The red aqua ion, $[Nb_4(\mu_4\text{-}S)(\mu_2\text{-}O)_5(H_2O)_{10}]^{4+}$, which elutes before the yellow-brown from a Dowex 50W-X2 cation-exchange column, has been characterized and reported in a preliminary communication.[7]

We report here further investigations on the $[Nb_4(\mu_4\text{-}S)(\mu_2\text{-}O)_5(H_2O)_{10}]^{4+}$ aqua ion along with characterization of the yellow-brown $[Nb_5(\mu_3\text{-}S)_2(\mu_3\text{-}O)_2(\mu_2\text{-}O)_2(H_2O)_{14}]^{8+}$ aqua ion.

Experimental Section

Starting Materials. All commercially available chemicals were used as received. Sodium thiocyanate (Aldrich, ReagentPlus, 99.99+%) and *p*-toluenesulfonic acid, HPTS (Aldrich, ACS reagent, ≥98.5%) were used. Lithium *p*-toluenesulfonate, LiPTS, was prepared by neutralizing HPTS with lithium carbonate and was then recrystallized twice from water. All preparations of Nb products and kinetics studies were carried out under an argon atmosphere. Synthesis of the Nb products was carried out in an efficient fume cupboard. Standard air-free techniques involving the use of argon, rubber septa, Teflon tubing and needles, and syringes as well as glovebag techniques were routinely employed in the manipulations.

Preparation of $[Nb_4(\mu_4\text{-}S)(\mu_2\text{-}O)_5(H_2O)_{10}]^{4+}$ and $[Nb_5(\mu_3\text{-}S)_2(\mu_3\text{-}O)_2(\mu_2\text{-}O)_2(H_2O)_{14}]^{8+}$. Niobium pentachloride (2 g) was dissolved in 30 mL of absolute ethanol, and the reduction was carried out using zinc powder (1 g). The solution turned from yellow to green and finally brown after several hours. After the solution reacted for 8 to 10 h, excess zinc was removed by filtration; the reduced mixture was added to 4 M HCl (120 mL), followed quickly by sodium sulfide nonahydrate (14 g). The reaction vessel was loosely stoppered, and the mixture was left to react with occasional shaking until the vigorous effervescence ceased. The resulting dark brown solution was filtered and purged with a vigorous stream of argon. After 3-fold dilution with water, the solution was adsorbed on a Dowex 50W-X2 cation-exchange column (2.2 cm × 45 cm). An uncharged brown species was removed by washing with 0.8 M HCl. Upon washing with copious amounts of 1 and 1.5 M HCl, red and green species separate from each other. The red species, the $[Nb_4(\mu_4\text{-}S)(\mu_2\text{-}O)_5(H_2O)_{10}]^{4+}$ aqua ion, eluted first in 2 M HCl, followed by the green $[Nb_3(\mu_3\text{-}Cl)(\mu_2\text{-}O_3)(H_2O)_9]^{4+}$ (hereafter, $Nb_3ClO_3^{4+}$). Sometimes, a small amount of the yellow $[Nb_2(\mu_2\text{-}S_2)_2(H_2O)_8]^{4+}$ aqua ion (hereafter, $Nb_2(S_2)_2^{4+}$) closely preceded these two species. The $Nb_3ClO_3^{4+}$ and $Nb_2(S_2)_2^{4+}$ species were identified by comparison of the observed and published UV−visible spectra.[4,5] Upon the column being washed with 3 M HCl, the highly charged yellow-brown aqua ion $[Nb_5(\mu_3\text{-}S)_2(\mu_3\text{-}O)_2(\mu_2\text{-}O)_2(H_2O)_{14}]^{8+}$ eluted. A dark brown band remained on the column and eluted very slowly with 4−5 M HCl. The red and yellow-brown aqua ions, which eluted in 2 and 3 M HCl, respectively, were collected and purified further by Dowex 50W-X2 column chromatography. Yields were typically ca. 12−15% and ca. 3−4% on the basis of niobium for the red and yellow-brown aqua ions, respectively. Solutions of the niobium aqua ions in HPTS can be obtained by exchanging HCl with HPTS on a cation-exchanger. However, much lower concentrations of niobium aqua ions in HPTS are obtained than in HCl, especially for the yellow-brown aqua ion, where the highest concentration achieved was typically only 1 mM per Nb in 4 M HPTS.

Analysis on $[Nb_5(\mu_3\text{-}S)_2(\mu_3\text{-}O)_2(\mu_2\text{-}O)_2(H_2O)_{14}]^{8+}$. The charge of the yellow-brown aqua ion was determined on a Dowex 50W-X2 cation-exchange column by using $[(H_2O)_9Mo_3S_4MoS_4Mo_3(H_2O)_9]^{8+}$ [8] as reference compound. It elutes after the reference compound, indicating a charge of at least 8+. The niobium and sulfur contents were determined by inductively coupled plasma atomic emission spectroscopy (ICP-AES). A Nb:S ratio of (2.47 ± 0.09):1 was obtained (average of four determinations). The oxidation state of Nb was determined by titration with $[Mo_4S_4(H_2O)_{12}]^{5+}$ (ϵ_{645} = 435 M^{-1} cm^{-1}; E^0 for $[Mo_4S_4(H_2O)_{12}]^{5+/4+}$ = −0.21 V vs NHE).[9] The reaction was monitored under an argon atmosphere by following the drop in absorbance at 645 nm. The reduced Mo product $[Mo_4S_4(H_2O)_{12}]^{4+}$ shows negligible absorbance at this wavelength, whereas the oxidized Nb(V) product is colorless and does not contribute to the absorbance. Measurements indicate a 1:5 $[Nb_5(\mu_3\text{-}S)_2(\mu_3\text{-}O)_2(\mu_2\text{-}O)_2(H_2O)_{14}]^{8+}$ to $[Mo_4S_4(H_2O)_{12}]^{5+}$ stoichiometry according to the equation

$$Nb(IV)_5 + 5Mo_4S_4^{5+} \rightarrow 5Mo_4S_4^{4+} + Nb(V)_5$$

The stoichiometry requires an oxidation state of +4 for all five Nb atoms.

Preparation of $(Me_2NH_2)_6[Nb_5S_2O_4(NCS)_{14}]\cdot 3.5H_2O$ (1). Crystals of **1** were obtained by adding solid KNCS (100 mg) to a solution of the yellow-brown $[Nb_5(\mu_3\text{-}S)_2(\mu_3\text{-}O)_2(\mu_2\text{-}O)_2(H_2O)_{14}]^{8+}$ aqua ion (5 mM per Nb, 2 mL) in 3 M HCl. The color of the solution turned immediately from yellow-brown to a darker brown. After the solution stood for an hour at room temperature, an aqueous solution of Me_2NH_2Cl (0.5 g in 1 mL water) was layered on the top. After the mixture stood at 4 °C for 2−3 days, dark brown rectangular block crystals of **1**, suitable for X-ray crystallography, deposited. Anal. Calcd for $C_{26}H_{55}N_{20}$ $Nb_5O_{7.50}$ S_{16}: C, 17.89; H, 3.18; N, 16.05. Found: C, 17.92; H, 3.21; N, 16.15. Yield: 14 mg (82%).

X-ray Crystallography. Crystal data are listed in Table 1. Under a protective layer of paraffin oil, a dark brown crystal was selected. The crystal was cooled to 120 K using a Cryostream nitrogen gas cooler system. The data were collected on a Siemens SMART platform diffractometer with a CCD area-sensitive detector. The structure was solved by direct methods and refined by full-matrix least-squares against F^2 of all data. Nine of the NCS groups are disordered; in seven of them, only the sulfur atoms split between

(4) Richens, T. R.; Shannon, I. J. *J. Chem. Soc., Dalton Trans.* **1998**, 2611.
(5) Sokolov, M. N.; Hernandez-Molina, R.; Elsegood, M. R.; Heath, S. L.; Clegg, W.; Sykes, A. G. *J. Chem. Soc., Dalton Trans.* **1997**, 2059.
(6) Ooi, B. L.; Søtofte, I. *Inorg. Chim. Acta* **2004**, *357*, 3780.
(7) Ooi, B. L.; Søtofte, I.; Bendtsen, M. F.; Munch, A.; Nielsen, L. C.; Henriksen, J. *Inorg. Chem.* **2005**, *44*, 480.
(8) Shibahara, T.; Yamamoto, T.; Kanadani, H.; Kuroya, H. *J. Am. Chem. Soc.* **1987**, *109*, 3495.
(9) Ooi, B. L.; Sharp, C.; Sykes, A. G. *J. Am. Chem. Soc.* **1989**, *111*, 125.

Table 1. Crystallographic Data for $(Me_2NH_2)_6[Nb_5S_2O_4(NCS)_{14}]\cdot 3.5H_2O$ (**1**)

formula	$C_{26}H5_5N_{20}\,Nb_5O_{7.5}\,S_{16}$
fw	1745.41
T (°C)	120(2)
cryst syst, color	monoclinic, dark brown
cryst dimension (mm^3)	$0.2 \times 0.12 \times 0.12$
space group	$P2_1/n$
a (Å)	15.4018(5)
b (Å)	21.1932(8)
c (Å)	22.0487(8)
β (deg)	103.459(1)
V ($Å^3$)	6999.3(4)
Z	4
D_c (g cm^{-3})	1.656
μ (Mo−K$_\alpha$, $\lambda = 0.71070$ Å) (mm^{-1})	1.322
θ range (deg)	1.75−28.00
no. of measured reflns	49 468
no. of unique reflns	16 660
no. of reflns with $I > 2\sigma(I)$	11434
R(int)	0.04(6)
transmission factors	1.0000−0.8494
no. of refined params	746
R_1 (obs. data)[a]	0.0659
wR_2 (all data)[b]	0.2033
GOF	1.036
max, min $\Delta\rho$ (e $Å^{-3}$)	1.883, −1.415

[a] $R_1 = \sum||F_o| - |F_c||/\sum|F_o|$. [b] $wR_2 = \sum w|F_o^2 - F_c^2|^2/\sum wF_o^4|^{1/2}$.

two positions, with population factors of 0.854(7) and 0.146(7) for S(2) and S(2)′, 0.93(2) and 0.07(2) for S(4) and S(4)′, 0.70(1) and 0.30(1) for S(6) and S(6)′, 0.766(6) and 0.234(6) for S(11) and S(11)′, 0.71(3) and 0.29(3) for S(13) and S(13)′, 0.562(5) and 0.438(5) for S(15) and S(15)′, and 0.78(1) and 0.22(1) for S(16) and S(16)′, respectively. In the last two groups, both the C and S atoms split between two positions, with population factors of 0.593(4) and 0.407(4) for C(8),S(10) and C(8)′,S(10)′ and 0.772(8) and 0.228(8) for C(12),S(14) and C(12)′,S(14)′, respectively. In all of the disordered NCS groups, the S atoms were refined with equal C−S bonds with an effective standard deviation 0.02. The temperature factors of some of the S and S′ atoms and some of the atoms in the cations are rather large and may indicate that the atoms are disordered. The water molecules are disordered with a population factor 0.5, and some may be even more disordered. Even though the cations and water molecules are disordered, the structure reported here is a reasonable model. The modifications of the positions and the population factors of the cations and the water molecules do not change the structure of the anion. The nonhydrogen atoms were refined anisotropically. The positions of the hydrogen atoms of the cations and water molecules were neither found nor calculated and therefore are not included in the refinement. The programs used for data collection, data reduction, and absorption were SMART, SAINT, and SADABS.[10,11] The SHELXTL 95[12] program was used to solve the structures and for molecular graphics.

EPR Spectroscopy. Spectra were recorded on a Bruker EMX spectrometer with a 12 kW 10 in. magnet equipped with a Bruker ER4102ST x-band cavity. Samples of the $[Nb_5(\mu_3\text{-}S)_2(\mu_3\text{-}O)_2(\mu_2\text{-}O)_2(H_2O)_{14}]^{8+}$ aqua ion were cooled to 90 K by quenching a standard EPR quartz tube (Wilmad) containing the sample into a glycerine-coated finger dewar, which was then placed directly in the cavity. The cavity was flushed continuously with inert gas in order to avoid water condensation and had a microwave frequency of 9.4019 GHz. EPR spectra of 36, 18, and 9 mM (per Nb) solutions of $[Nb_5(\mu_3\text{-}S)_2(\mu_3\text{-}O)_2(\mu_2\text{-}O)_2(H_2O)_{14}]^{8+}$ were obtained. An attempt to record an EPR spectrum of the sample was also carried out at room temperature.

Kinetic Studies on the 1:1 Equilibration of NCS^- with $Nb_4(\mu_4\text{-}S)(\mu_2\text{-}O)_5(H_2O)_{10}]^{4+}$ and $[Nb_5(\mu_3\text{-}S)_2(\mu_3\text{-}O)_2(\mu_2\text{-}O)_2(H_2O)_{14}]^{8+}$. All runs were carried out in HPTS at 25.0 ± 0.1 °C, and I was adjusted to 2.00 M (LiPTS). The $[Nb_4(\mu_4\text{-}S)(\mu_2\text{-}O)_5(H_2O)_{10}]^{4+}$ and $[Nb_5(\mu_3\text{-}S)_2(\mu_3\text{-}O)_2(\mu_2\text{-}O)_2(H_2O)_{14}]^{8+}$ aqua ions (hereafter, $Nb_4SO_5^{4+}$ and $Nb_5S_2O_4^{8+}$, respectively) were eluted from Dowex 50W-X2 cation-exchange columns with 4 M HPTS and stock solutions stored under argon atmosphere. Stopped-flow spectrophotometry on a Hi-Tech PQ/SF-53 instrument was employed for the reactions of both $Nb_4SO_5^{4+}$ and $Nb_5S_2O_4^{8+}$ with NCS^-. The reaction of $Nb_4SO_5^{4+}$ with NCS^- was monitored at 380 nm with both NCS^- and metal complex in ≥10-fold excess. The concentration of NCS^- was restricted to ≤4 mM to avoid formation of the higher thiocyanato complexes. The reaction of $Nb_5S_2O_4^{8+}$ with NCS^- was monitored at 390 nm with only NCS^- in excess. Rate constants were obtained using fitting procedures from On-Line Instrument Systems (OLIS, Bogart, GA). Unweighted linear least-squares fitting procedures were used in the treatment of data.

Computational Studies. Spin-restricted density functional calculations (DFT) were carried out on the different model complexes using the Amsterdam density functional (ADF2002) program.[13] The VWN parameterization was used for the local density approximation (LDA),[14] with gradient corrections (GGA) added for exchange (Becke88)[15] and correlation (Perdew).[16] The relativistic corrections for all atoms were accounted for by the scalar ZORA (zeroth-order relativistic approximation) method.[17] The standard ADF TZP basic set was used for all of the atoms. The frozen core approximation was used to treat the core electrons of Nb (1s4p), S (1s2p), O (1s), N (1s), C (1s), and Cl (1s2p). The symmetrized atomic coordinates (C_{2v} symmetry) from X-ray structures of $Cs_{4.67}Na_{1.33}[Nb_4SO_5(NCS)_{10}]\cdot 2.33H_2O$[7] and $(Me_2NH_2)_6[Nb_5S_2O_4(NCS)_{14}]\cdot 3.5H_2O$ (**1**) were used as starting atomic coordinates in the calculations. The atomic net charges were calculated using the Hirshfeld analysis.[18] The fragment interaction analysis was done using the method proposed by Ziegler.[19] According to this method, the bonding energy (E_{total}) between two fragments can be decomposed into two terms. One is called the steric repulsion energy (E_{ster}); it is sum of the attractive electrostatic interactions (ionicity) and the repulsive two-orbital, four-electron interactions (Pauli destabilization) between occupied orbitals on both fragments. The other term represents the stabilizing electronic interaction energy due to orbital interactions (E_{orbit}) between vacant and occupied fragment orbitals (the covalent bonding interactions).

(10) *SMART and SAINT, Area Detector Control and Integration Software*, version 5.054; Bruker Analytical X-ray Instruments Inc.: Madison, WI, 1998.

(11) Sheldrick, G. M. *SADABS, Program for Empirical Correction of Area Detector Data*, version 2.03; University of Göttingen: Göttingen, Germany, 2001.

(12) Sheldrick, G. M. *SHELXTL, Structure Determination Programs*, version 6.12; Bruker Analytical X-ray Instruments Inc.: Madison, WI, 2001.

(13) *Amsterdam Density Functional (ADF) Program*, release 2002.02; Vrije Universteit: Amsterdam, 2002. Te-Velde, G. F.; Bickelhaupt, M. E.; Baerends, J.; Fonseca Guerra, C.; Van-Gisbergen, S. J A.; Snijders, J.G.; Ziegler, T. *J. Comput. Chem.* **2001**, *22*, 931.

(14) Vosko, S. H.; Wilk, L.; Nusair, M. *Can. J. Phys.* **1980**, *58*, 1200−1211.

(15) Becke, A. D. *Phys. Rev. A.* **1988**, *38*, 3098−3100.

(16) Perdew, J. P. *Phys. Rev. B.* **1986**, *33*, 8822−8824.

(17) Van Lenthe, E.; Ehlers, A.; Baerends, E. J. *J. Chem. Phys.* **1999**, *110*, 8943−8953.

(18) Hirshfeld, F. L. *Theor. Chim. Acta* **1977**, *44*, 129−138.

(19) Ziegler, T.; Rauk, A.; Baerends, E. J. *Theor. Chim. Acta* **1977**, *43*, 261. Ziegler, T. *Metal Ligand Interactions: From Atoms to Clusters to Surfaces*; Salahub, D. R., Russo, N., Eds.; Kluwer: Dordrecht, The Netherlands, 1992; p 367.

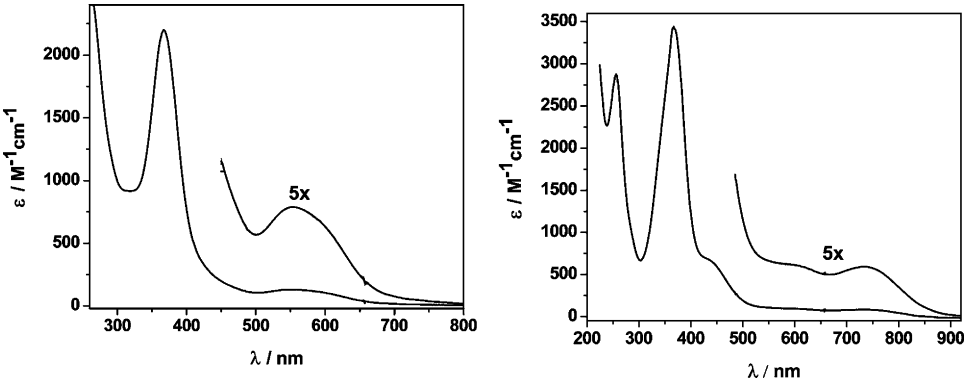

Figure 1. Electronic spectra of $[Nb_4(\mu_4\text{-}S)(\mu_2\text{-}O)_5(H_2O)_{10}]^{4+}$ in 2 M HCl (left) and $[Nb_5(\mu_3\text{-}S)_2(\mu_3\text{-}O)_2(\mu_2\text{-}O)_2(H_2O)_{14}]^{8+}$ in 3 M HCl (right).

Results

Properties of $Nb_4SO_5^{4+}$ and $Nb_5S_2O_4^{8+}$. In 2 M HCl, $Nb_4SO_5^{4+}$ has λ_{max} at 369 nm ($\epsilon = 2200$ M^{-1} cm^{-1} per Nb) and 555 nm ($\epsilon = 145$ M^{-1} cm^{-1} per Nb) and a slight shoulder at ca. 600 nm, whereas in 2 M HPTS, the peaks shift to 365 nm (2560 M^{-1} cm^{-1} per Nb) and 550 nm (130 M^{-1} cm^{-1} per Nb). The $Nb_5S_2O_4^{8+}$ ion shows λ_{max} peaks at 369 nm ($\epsilon = 3470$ M^{-1} cm^{-1} per Nb) and 735 nm ($\epsilon = 105$ M^{-1} cm^{-1} per Nb) and shoulders at 440 nm ($\epsilon = 705$ M^{-1} cm^{-1} per Nb) and 600 nm ($\epsilon = 110$ M^{-1} cm^{-1} per Nb) in 3 M HCl, whereas in 4 M HPTS, they appear at 365 nm ($\epsilon = 4000$ M^{-1} cm^{-1} per Nb) and 725 nm ($\epsilon = 98$ M^{-1} cm^{-1} per Nb) and 435 nm ($\epsilon = 780$ M^{-1} cm^{-1} per Nb), and 590 nm ($\epsilon = 101$ M^{-1} cm^{-1} per Nb). The electronic spectra of both aqua ions are shown in Figure 1. Solutions of both species (ca. 1−2 mM) show ca. 80−90% decay in absorbance at 369 nm after ≤ 2 h exposure to air with intermittent shaking.

The $Nb_4SO_5^{4+}$ aqua ion eluted as a 4+ species on a Dowex-50W-X2 cation-exchange column, after reference $[Mo_3S_4(H_2O)_9]^{4+}$ but before $[Mo_4S_4(H_2O)_{12}]^{5+}$. The charge of the yellow-brown aqua ion was determined to be 8+ on the basis of the elution behavior, whereby it eluted after the well-characterized $[(H_2O)_9Mo_3S_4MoS_4Mo_3(H_2O)_9]^{8+}$ aqua ion.[8] The oxidation state of +4 for all five Nb atoms together with the ICP-AES analyses, the overall charge of 8+, and X-ray structure of the thiocyanate derivative (see below) support a formula of $Nb_5S_2O_4^{8+}$. Both aqua ions do not give 100% recovery from Dowex cation-exchange columns, whereby a dark brown material always remained on the top. The percentage of the recovery depends on factors such as concentration of H^+ during loading, whether the coordinating HCl or noncoordinating HPTS was employed, and the duration of the chromatographic procedure. The chromatographic behavior suggests that hydrolytic polymerization could be severe.

Thiocyanate complex $(Me_2NH_2)_6[Nb_5S_2O_4(NCS)_{14}]\cdot 3.5H_2O$ (**1**) was isolated in high yield from 3 M HCl solutions of $Nb_5S_2O_4^{8+}$ in the presence of KSCN and Me_2NH_2Cl.

$$[Nb_5(\mu_3\text{-}S)_2(\mu_3\text{-}O)_2(\mu_2\text{-}O)_2(H_2O)_{14}]^{8+} + 14KSCN + 6Me_2NH_2Cl \rightarrow (Me_2NH_2)_6[Nb_5S_2O_4(NCS)_{14}] + 14H_2O + 6KCl + 8K^+ \quad (1)$$

Upon exposure to air, dark brown crystals of the thiocyanate complex eventually turned to a yellow-orange solid.

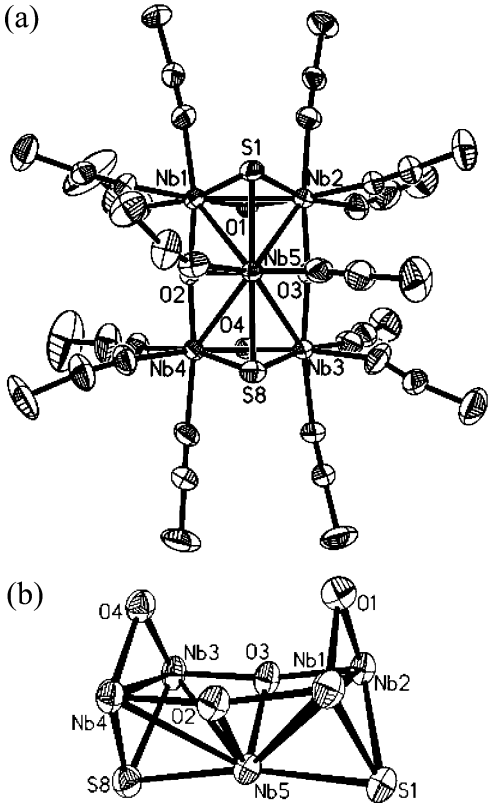

Figure 2. (a) Perspective view of $[Nb_5(\mu_3\text{-}S)_2(\mu_3\text{-}O)_2(\mu_2\text{-}O)_2(NCS)_{14}]^{6-}$ anion. The thermal ellipsoids are drawn at a 50% probability level. (b) View of the $Nb_5(\mu_3\text{-}S)_2(\mu_3\text{-}O)_2(\mu_2\text{-}O)_2^{8+}$ core comprising two $Nb(\mu_3\text{-}S)(\mu_2\text{-}O)_3$ units fused together at the O2−Nb5−O3 face. The five Nb atoms are arranged in a folded bow tie conformation.

X-ray Crystal Structure of $(Me_2NH_2)_6[Nb_5S_2O_4(NCS)_{14}]\cdot 3.5H_2O$ (1). The X-ray structural analysis of **1** prepared from the reaction of the yellow-brown aqua ion with thiocyanate revealed an unprecedented pentanuclear core structure, $Nb_5(\mu_3\text{-}S)_2(\mu_3\text{-}O)_2(\mu_2\text{-}O)_2^{8+}$, in the $[Nb_5(\mu_3\text{-}S)_2(\mu_3\text{-}O)_2(\mu_2\text{-}O)_2(NCS)_{14}]^{6-}$ anion (Figure 2). Selected bond distances and angles are given in Table 2.

Two types of Nb atoms are present, one of the first type and four of the second. Ignoring Nb−Nb bonds, the geometry of Nb is distorted octahedral in both cases. The first type of Nb (Nb5) atom is bonded to two NCS^-, two μ_3-S and two μ_3-O, whereas each of the second type of Nb (Nb1, Nb2, Nb3 and Nb4) atom is bonded to three NCS^-, one μ_3-S, one μ_3-O, and one μ_2-O. The five Nb atoms are arranged in a folded bow tie configuration, as depicted in Figure 2. Nb1,

Table 2. Selected Bond Distances (Å) and Bond Angles (deg) in $[Nb_5(\mu_3\text{-}S)_2(\mu_3\text{-}O)_2(\mu_2\text{-}O)_2(NCS)_{14}]^{6-}$

Nb(1)−Nb(2)	2.7995(8)	Nb(1)−S(1)−Nb(2)	70.71(5)
Nb(3)−Nb(4)	2.8064(8)	Nb(3)−S(8)−Nb(4)	70.63(5)
Nb(1)−Nb(5)	2.9108(8)	Nb(1)−S(1)−Nb(5)	72.61(5)
Nb(2)−Nb(5)	2.9111(8)	Nb(2)−S(1)−Nb(5)	72.74(5)
Nb(3)−Nb(5)	2.8923(8)	Nb(3)−S(8)−Nb(5)	71.84(5)
Nb(4)−Nb(5)	2.8930(8)	Nb(4)−S(8)−Nb(5)	72.08(5)
Nb(1)−S(1)	2.4229(17)	Nb(1)−O(1)−Nb(2)	86.75(17)
Nb(2)−S(1)	2.4153(17)	Nb(3)−O(4)−Nb(4)	87.63(17)
Nb(3)−S(8)	2.4339(18)	Nb(1)−O(2)−Nb(5)	91.26(17)
Nb(4)−S(8)	2.4208(19)	Nb(4)−O(2)−Nb(5)	90.31(17)
Nb(5)−S(1)	2.4927(17)	Nb(2)−O(3)−Nb(5)	91.55(17)
Nb(5)−S(8)	2.4955(18)	Nb(3)−O(3)−Nb(5)	90.65(17)
Nb(1)−O(1)	2.037(4)		
Nb(2)−O(1)	2.039(4)		
Nb(3)−O(4)	2.019(5)		
Nb(4)−O(4)	2.034(4)		
Nb(1)−O(2)	1.946(4)		
Nb(4)−O(2)	1.955(4)		
Nb(2)−O(3)	1.951(4)		
Nb(3)−O(3)	1.956(4)		
Nb(5)−O(2)	2.122(4)		
Nb(5)−O(3)	2.108(4)		

Table 3. Average Values of Selected Bond Lengths (Å) and Angles (deg)

Nbn−Nb(n+1) (n = 1, 3)	2.803(4)
Nb5−Nbn (n = 1, 2)	2.9110(2)
Nb5−Nbn (n = 3, 4)	2.8926(4)
Nbn−μ_3-S (n = 1−4)	2.423(4)
Nb5−μ_3-S	2.494(1)
Nbn−μ_2-O (n = 1−4)	2.034(4)
Nbn−μ_3-O (n = 1−4)	1.952(2)
Nb5−μ_3-O	2.115(7)
Nbn−μ_3-S−Nb(n + 1) (n = 1, 3)	70.67(4)
Nb5−μ_3-S−Nbn (n = 1−4)	72.3(2)
Nbn−μ_2-O−Nb(n + 1) (n = 1, 3)	87.2(4)
Nb5−μ_3-O−Nbn (n = 1−4)	90.9(3)

Nb2, Nb3, and Nb4 form a rectangular plane. Two O atoms, O2 and O3, are nearly coplanar with this rectangular plane, being slightly displaced by 0.1 Å toward Nb5. The Nb5 core can be considered as consisting of two triangular $Nb_3(\mu_3\text{-}S)(\mu_2\text{-}O)_3$ units of the type previously seen in the $[Nb_3SO_3(NCS)_9]^{6-}$ anion. The two $Nb_3(\mu_3\text{-}S)(\mu_2\text{-}O)_3$ units are fused together by sharing a triangular (μ_2-O)−Nb−(μ_2-O) face that contains O2, Nb5, and O3.

The formal oxidation state of Nb in the cluster is Nb(IV) (d^1 electron configuration), with five electrons involved in the formation of six Nb−Nb bonds; the Nb−Nb bond order is 5/12. The average Nbn−Nb(n + 1) (n = 1, 3) bond distance of 2.803(4) Å is significantly shorter than the average Nb5−Nbn (n = 1, 2) and Nb5−Nbn (n = 3, 4) bond distances of 2.9110(2) and 2.8926(4) Å, respectively, Table 3. It must be borne in mind that the metal−metal bond distances depend not only on the bond order but also strongly on the nature, size, and arrangement of the bridging ligands. In this case, the unique Nb5 is bridged to the other Nb atoms by two flattened μ_3−O groups, O2 and O3. This imposes geometrical constraints and deformation to Nb5, as reflected in the Nb5−O and Nb5−S distances as well. All Nb−Nb bond distances are longer than those of the Nb(III)(IV)$_2$ cluster, $[Nb_3SO_3(NCS)_9]$,$^{6-}$ where the average Nb−Nb distance is 2.763(3) Å and Nb−Nb bond order is 2/3 (four electrons involved in the formation of three Nb−Nb bonds).[3] However, a large spread of Nb−Nb distances have previously been observed, particularly for triangular niobium cluster complexes; for example, 2.807(4) Å in $[Nb_3(\mu\text{-}Cl)_2(\mu\text{-}OH)(\mu\text{-}O)_3(\eta^5\text{-}C_5Me_5)_3]^+$,[20] 2.833(7) Å in $[Nb_3(\mu_3\text{-}O)_2(\mu\text{-}O_2CMe)_6(thf)_3]^+$,[21] 2.857(5) Å in $[Nb_3(\mu\text{-}Cl)_3(\mu\text{-}O)_3(\eta^5\text{-}C_5Me_5)_3]^+$,[20] 2.870(6) and 2.885(5) Å in $[Nb_3(\mu_3\text{-}O)_2(\mu\text{-}SO_4)_6(H_2O)_3]$,[5−21,22] 2.976(6) Å in $[Nb_3(\mu_3\text{-}Cl)(\mu_2\text{-}Cl)_3Cl_6(PEt_3)_3]^-$,[23] and 3.140(4) Å in $[Nb_3(\mu\text{-}O)_2(\mu\text{-}OH)_2(\mu\text{-}O_2CMe)_3(\eta^5\text{-}C_5Me_5)_3]$.[24]

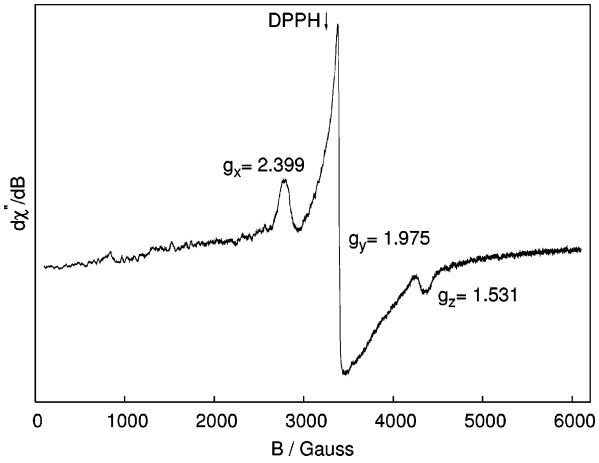

Figure 3. EPR spectrum of $[Nb_5(\mu_3\text{-}S)_2(\mu_3\text{-}O)_2(\mu_2\text{-}O)_2(H_2O)_{14}]^{8+}$ in frozen aqueous 4 M HCl (36 mM per Nb). The sample was quenched in liquid-nitrogen-containing finger dewar.

EPR Spectroscopy. The spectrum of the quenched frozen solution of the 36 mM solution of $Nb_5S_2O_4^{8+}$ aqua ion is shown in Figure 3. The spectrum shows, in correlation with the structure of the corresponding thiocyanate derivative, that the molecule has total anisotropy (C_{2v}); thus, all three tensors ($\mathbf{g}_x$,= 2.399, $\mathbf{g}_y$ = 1.975, and $\mathbf{g}_z$ = 1.531) can be resolved. No hyperfine interaction expected from the nuclear moment of I = 9/2 for ^{93}Nb (100% abundance) was observed. To verify whether this phenomenon is due to increased spin−spin relaxation and therefore proportional to the concentration of the clusters in aqueous solution, we obtained a series of the spectra with decreasing concentrations of $Nb_5S_2O_4^{8+}$ (36, 18, and 9 mM per Nb). Decreasing the concentration of $Nb_5S_2O_4^{8+}$ in solution did not induce resolution of the hyperfine structure but merely a decrease in spin numbers as a function of concentration. Thus, the collapse of the hyperfine multiplet must arise from the interaction between the niobium nuclei inside the clusters, which forces the nuclear spins to align. Aqueous solutions of $Nb_5S_2O_4^{8+}$ do not give any EPR signal at room temperature.

Kinetic Studies. Kinetics of 1:1 Equilibration of NCS$^-$ with $Nb_4SO_5^{4+}$. With NCS$^-$ in a large (>10-fold) excess of $Nb_4SO_5^{4+}$, biphasic kinetics was observed. Upon a variation in the concentration of NCS$^-$, rate constants for one phase

(20) Bottomley, F.; Karslioglu, S. *J. Chem. Soc., Chem. Commun.* **1991**, 222.
(21) Cotton, F. A.; Diebold, M. P.; Roth, W. J. *Inorg. Chem,* **1988**, *27*, 2347.
(22) Bino, A. *Inorg. Chem.* **1982**, *21*, 1917.
(23) Cotton, F. A.; Diebold, M. P.; Feng, X.; Roth, W. J. *Inorg. Chem,* **1988**, *27*, 3414.
(24) Kalinnikov, V. T.; Pasynskii, A. A.; Larin, G. M.; Novotortsev, Yu. V. M.; Struchkov, T.; Gusev, A. I.; Kirillova, N. I. *J. Organomet. Chem.*, **1974**, *74*, 91.

Table 4. Rate Constants k_{eq} at 25 °C for the Reaction of $[Nb_4(\mu_4\text{-}S)(\mu_2\text{-}O)_5(H_2O)_{10}]^{4+}$ with NCS^-, $I = 2.00$ M (LiPTS)

[HPTS] (M)	[NCS^-] (mM)	[$Nb_4SO_5]^{4+}$ (mM per Nb)	$10^2 \cdot k_{eq}$ (s^{-1})
0.50	4.00	0.25	6.09
1.00	3.50	0.20	6.17
2.00	1.50	0.15	3.79
2.00	2.50	0.25	5.14
2.00	3.00	0.25	5.40
2.00	3.20	0.25	5.60
2.00	4.00	0.25	6.34
2.00	0.20	2.37	4.87

assigned as the first-order equilibration rate constants (k_{eq}) show a linear dependence on [NCS^-]. The rate constants k_{eq} at 25 °C are independent of [H^+] in the range 0.5−2.0 M, Table 4. One run with $Nb_4SO_5^{4+}$ in excess showed only one phase, and the rate constant obtained corresponds best to k_{eq} with NCS^- in excess only if a statistical factor of 4 is allowed for, Figure 4. The linear dependences of k_{eq} on [NCS^-] can be expressed in terms of formation (k_f) and aquation (k_{aq}) rate constants, as in eq 1.

$$k_{eq} = k_f[NCS^-] + k_{aq} \quad (1)$$

The slope for the data in Figure 4 gives $k_f = 9.5\ M^{-1}\ s^{-1}$ and $k_{aq} = 2.6 \times 10^{-2}\ s^{-1}$; a formation constant K of 365 M^{-1} is obtained from k_f/k_{aq}. Because of the very small absorbance changes (<10 milliabsorbance units) for the second phase, rate constants are unreliable and show a large scatter, with no discernible dependence on [NCS^-]. It could be due to the isomerization of S-bonded Nb−SCN to N-bonded Nb−NCS or to positional isomerization (NCS^- reequilibrating to give occupancy at different sites) previously put forward for $[W_3S_4(H_2O)_9]^{4+}$ aqua ion,[25] but no further attempts were made to further investigate this phenomenon.

Kinetics of 1:1 Equilibration of NCS^- with $Nb_5S_2O_4^{8+}$. Because of the small absorbance changes and a high background absorbance, along with the rather low concentrations of $Nb_5S_2O_4^{8+}$ that can be achieved in HPTS, only limited kinetic data have been obtained. Under these constraints, measurements with Nb complex in excess are totally excluded, whereas runs with NCS^- in large (>10-fold) excess were accessible only for concentrations of [NCS^-] ≥ 2 mM. Biphasic kinetics was observed, and equilibration rate constants k_{eq} are obtained. Because of large errors observed, rate constants for the second phase are not further evaluated. With higher concentrations of [NCS^-] > 4 mM (where contributions from the formation of higher thiocyanato complexes cannot be ruled out), equilibration rate constants k_{eq} show clear signs of leveling off, Table 5 and Figure 5. With the rather high positive charge on $Nb_5S_2O_4^{8+}$, an Eigen−Wilkins mechanism is relevant for the reaction with NCS^-. Assuming saturation kinetics, a value of 0.2 s^{-1} is estimated for ligand substitution within the ion pair.

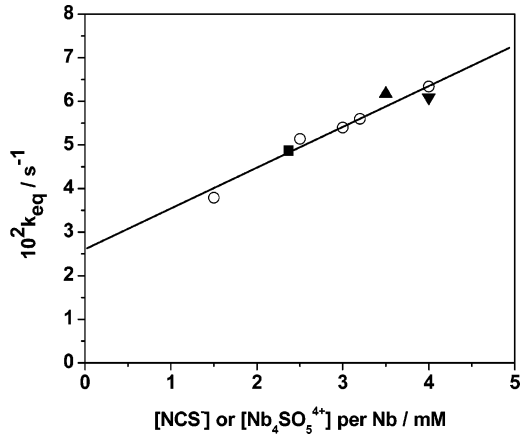

Figure 4. Dependence of equilibration rate constants k_{eq} (25 °C) on [NCS^-] or $[Nb_4SO_5^{4+}]$ for the reaction of $[Nb_4(\mu_4\text{-}S)(\mu_2\text{-}O)_5(H_2O)_{10}]^{4+}$ with NCS^-, $I = 2.0$ M (LiPTS). Runs with NCS^- in excess at [H^+] = 0.5 (▼), 1.00 (▼), and 2.00 M (○) and those with $Nb_4SO_5^{4+}$ in excess at [H^+] = 2.00 M (■).

Table 5. Rate Constants k_{eq} at 25°C for the Reaction of $[Nb_5(\mu_3\text{-}S)_2(\mu_3\text{-}O)_2(\mu_2\text{-}O)_2]^{8+}$ with NCS^-, $I = 2.00$ M (HPTS)

[NCS^-] (mM)	$[Nb_5S_2O_4^{8+}]$ (mM per Nb)	$10^2 \cdot k_{eq}$ (s^{-1})
2.50	0.25	15.0
4.00	0.25	18.8
6.00	0.30	19.5
7.00	0.30	19.4

Electronic Structures. Full geometry optimizations were performed for the $Nb_4SO_5^{4+}$ and $Nb_5S_2O_4^{8+}$ naked metal clusters (without external ligands) and for the $[Nb_4SO_5(NCS)_{10}]^{6-}$ and $[Nb_5S_2O_4(NCS)_{14}]^{6-}$ cluster complexes. The analysis of the interaction between the fragments of atoms in the optimized structures showed that E_{tot} has negative values for all of the model cations and anions, with the exception of $Nb_5S_2O_4^{8+}$. The naked $Nb_5O_4S_2^{8+}$ cluster is not stable on its own, but covalent bonding interactions (E_{orbit}) with the ligands lead to stable derivatives of it (Table 6). Additional fragmental analysis shows that the energy contributions (E_{tot}) are −35 and −150 eV for the interactions ($10NCS^- + Nb_4O_5S^{4+}$) and ($14NCS^- + Nb_5O_4S_2^{8+}$), respectively. The corresponding E_{orb} values are −90 and −280 eV, respectively. Essential covalent bonding in both complexes leads to relatively low atomic charges (Table 7).

The highest occupied molecular orbitals (HOMOs) and lowest unoccupied molecular orbitals (LUMOs) of the naked metal clusters, their symmetries, and their compositions are shown in Figures 6 and 7. Both HOMOs and LUMOs are largely centered on the niobium atoms. The $11b_2$ (HOMO) of $Nb_4O_5S^{4+}$ is a nondegenerate fully filled MO with essentially bonding character within the Nb2−Nb1−Nb2A

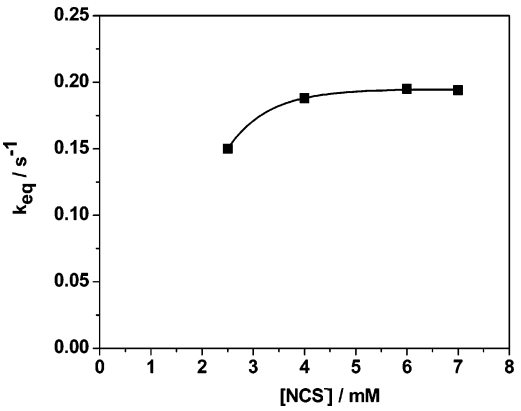

Figure 5. Dependence of equilibration rate constants k_{eq} (25 °C) on [NCS^-] for the reaction of the $[Nb_5(\mu_3\text{-}S)_2(\mu_3\text{-}O)_2(\mu_2\text{-}O)_2]^{8+}$ with NCS^-, $I = 2.00$ M (HPTS).

Table 6. Decomposition of the Bonding Energy (eV) for the Model Complexes

			E_{ster}		
	E_{tot}	E_{orbit}	Pauli	electronic	sum
$Nb_4O_5S^{4+}$	−27.04	−134.00	175.06	−68.11	106.95
$Nb_5O_4S_2^{8+}$	80.64	−9.65	151.23	−60.94	90.28
$[Nb_4O_5S(NSC)_{10}]^{6-}$	−281.98	−1070.48	1044.03	−255.53	788.50
$[Nb_5O_4S_2(NSC)_{14}]^{6-}$	−378.11	−1478.09	1459.84	−359.86	1099.99

Table 7. Calculated Atomic Charges (q/e) in the Model Complexes

	Nb	O	S	NCS
$Nb_4O_5S^{4+}$	1.32 (2)	−0.18 (4)	0.10	
	1.07 (2)	−0.15		
$Nb_5O_4S_2^{8+}$	1.70 (4)	−0.24 (2)	0.46 (2)	
	0.96	−0.10 (2)		
$[Nb_4O_5S(NSC)_{10}]^{6-}$	0.66 (2)	−0.38 (4)	−0.26	−0.66 (2); −0.62 (4)
	0.67 (2)	−0.37		−0.68 (2); −0.68 (2)
$[Nb_5O_4S_2(NSC)_{14}]^{6-}$	0.67 (4)	−0.33 (2)	−0.19 (2)	−0.52 (2); −0.54 (4)
	0.43	−0.33 (2)		−0.57 (4); −0.49 (4)

and Nb2−Nb3−Nb2A triangles and also between O1−Nb1-(Nb2), O1A−Nb1(Nb2A), O3A−Nb3(Nb2A), O3−Nb2-(Nb3), and S−Nb1(Nb3); however, it is essentially antibonding with respect to the O2−Nb2(Nb2A) interaction. The $16a_1$ (LUMO) has mixed (bonding and antibonding) character; the bonding is available between Nb2−Nb2A, O2−Nb2(Nb2A), Nb2−O1(O3), Nb2A−O1A(O3A), and S−Nb1-(Nb3). The calculated HOMO−LUMO gap is 1.35 eV. The $9a_2$ (HOMO) of $Nb_5O_4S_2^{8+}$ is a nondegenerate partially filled MO, antibonding between Nb2−Nb1 and Nb3−Nb4, with only a very small contribution from the Nb5 atom and zero contribution from S and O atoms. The $11b_1$ (LUMO) is a

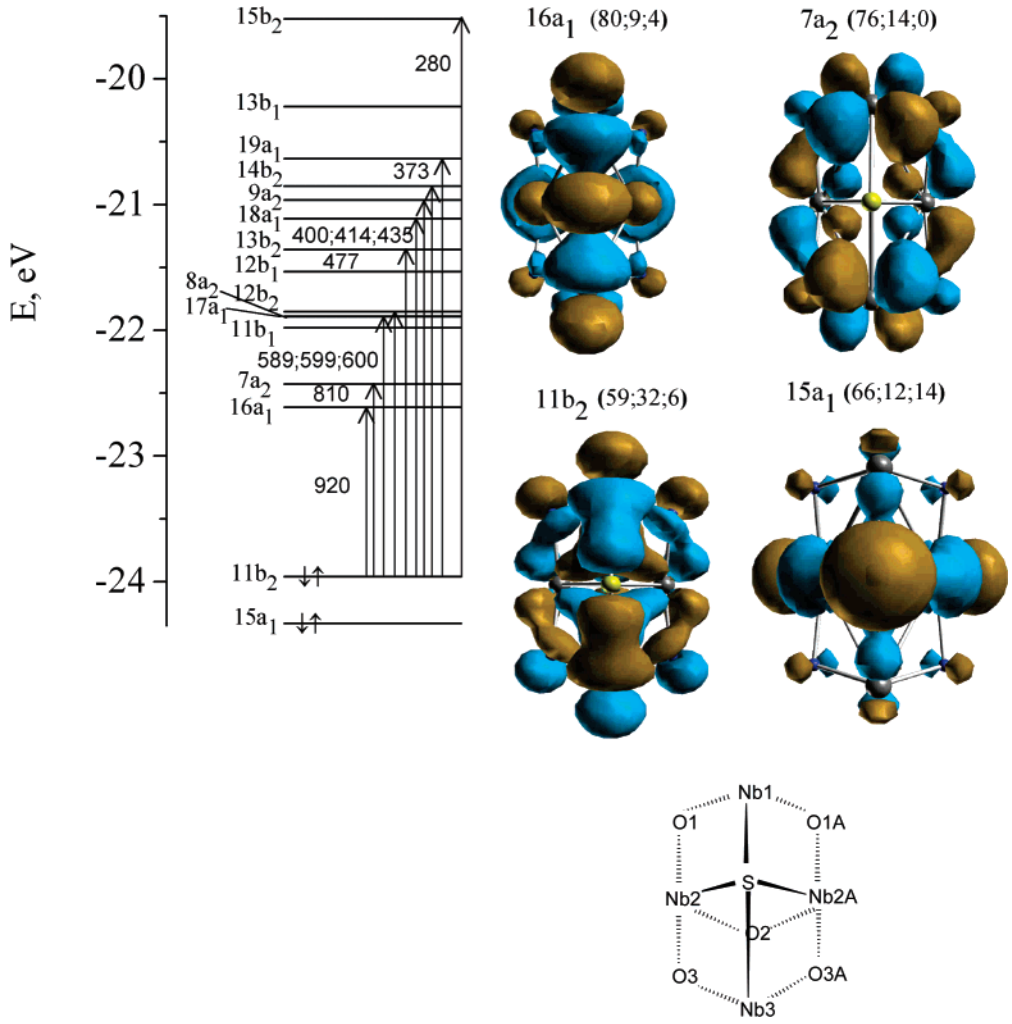

Figure 6. Schematic electronic levels and figures of MOs for C_{2v} $Nb_4SO_5^{4+}$. Indicated are the numbers and symmetry types of the calculated MOs. Numbers in brackets indicate the percentage of the contributing valence orbitals 4d Nb, 2p O, and 3p S, respectively (other metal and ligand s, p, and d contributions are negligible). The vertical arrows and integers (nm) show the calculated transitions. Sketch of the cluster is shown on the right (Nb−Nb bonding omitted).

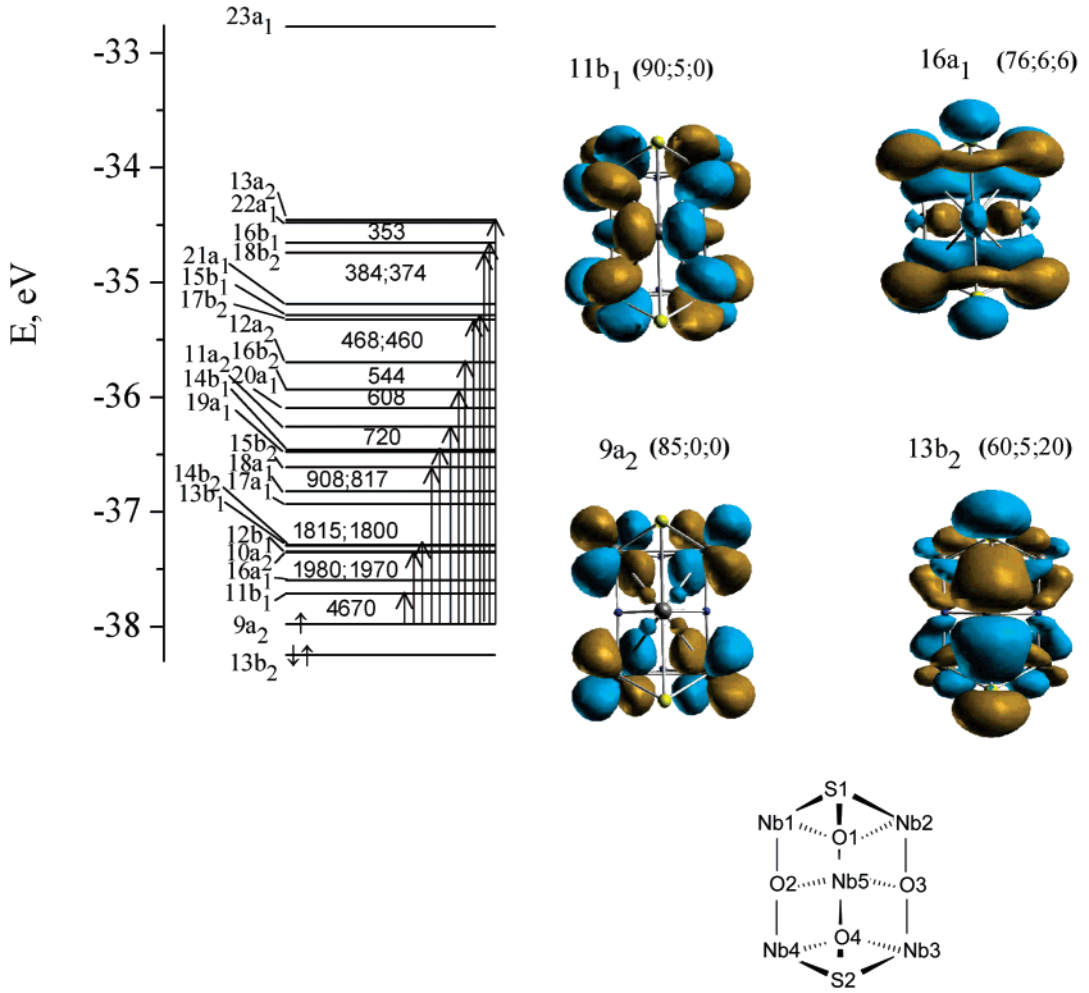

Figure 7. Schematic electronic levels and figures of MOs for C_{2v} $Nb_5S_2O_4^{8+}$. Indicated are the numbers and symmetry types of the calculated MOs. Numbers in brackets indicate the percentage of the contributing valence orbitals 4d Nb, 2p O, and 3p S, respectively (other metal and ligand s, p, and d contributions are negligible). The vertical arrows and integers (nm) show the calculated transitions. Sketch of the cluster is shown on the right (Nb−Nb bonding omitted).

nondegenerate MO, with essentially antibonding interaction between atoms; however, bonding is available between Nb5−O2(O3). The calculated HOMO−LUMO gap is 0.27 eV. This small value probably explains the instability of the naked $Nb_5O_4S_2^{8+}$ cluster.

To check the validity of our calculations, we compared the calculated orbital energies with the experimental UV−visible spectra. We supposed that the observed spectra originate from the excitations of the dipole electronic transitions from HOMO to vacant MO (the first order of approach). For a system with C_{2v} symmetry, the dipole-allowed excitations are those from a_2 to a_2, b_1, and b_2 levels, and from b_2 to a_1, a_2, and b_2 levels. Figures 6 and 7 show the calculated transitions. These values are in a qualitative agreement with the experimental UV−visible spectra.

The HOMO and LUMO of $[Nb_5O_4S_2(NCS)_{14}]^{6-}$ consist mainly of MOs of the naked $Nb_5O_4S_2^{8+}$ cluster (Figure 8). This complex must have paramagnetic properties, because the HOMO ($46a_1$) is partially filled; this is indeed supported by EPR spectroscopy. The calculated HOMO−LUMO gap is 0.28 eV. The arrangement of frontier orbitals of $Nb_5O_4S_2^{8+}$ is modified upon ligand coordination.

Discussion. Two unprecedented Nb(IV) aqua ions have been prepared by acid hydrolysis of zinc-reduced solutions of $NbCl_5$ in the presence of sulfide. One of them, the tetranuclear aqua ion, has been reported in a preliminary communication. Here, X-ray structure analysis of $(Me_2NH_2)_6[Nb_5S_2O_4(NCS)_{14}]\cdot 3.5H_2O$ prepared from the reaction of thiocyanate with the second aqua ion, together with ICP-AES analyses and oxidation-state and charge determination of the aqua ion, supports the existence of the pentanuclear $Nb_5S_2O_4^{8+}$ ion in solution. The structures of $[Nb_5(\mu_3\text{-}S)_2(\mu_3\text{-}O)_2(\mu_2\text{-}O)_2(NCS)_{14}]^{6-}$ and $[Nb_4(\mu_4\text{-}S)(\mu_2\text{-}O)_5(NCS)_{10}]^{6-}$ revealed totally new cluster types that are electron deficient, with Nb−Nb bonds of bond order less than one. The triangular $M_3(\mu_3\text{-}X)(\mu_2\text{-}X)_3$ unit, which dominates the aqueous chemistry of Mo, emerged as an important entity for Nb as well, where the triangular units fused to form clusters of higher nuclearity. The formation of clusters of higher nuclearity is a well-documented phenomenon for Cr(III). Hydrolytic oligomerization of Cr(III) results in the formation of a tetramer as one of the oligomeric products. The tetranuclear oxo/hydroxo complex $[Cr_4O(OH)_5(H_2O)_{10}]^{5+}$ had been proposed as one plausible tetrameric product. This

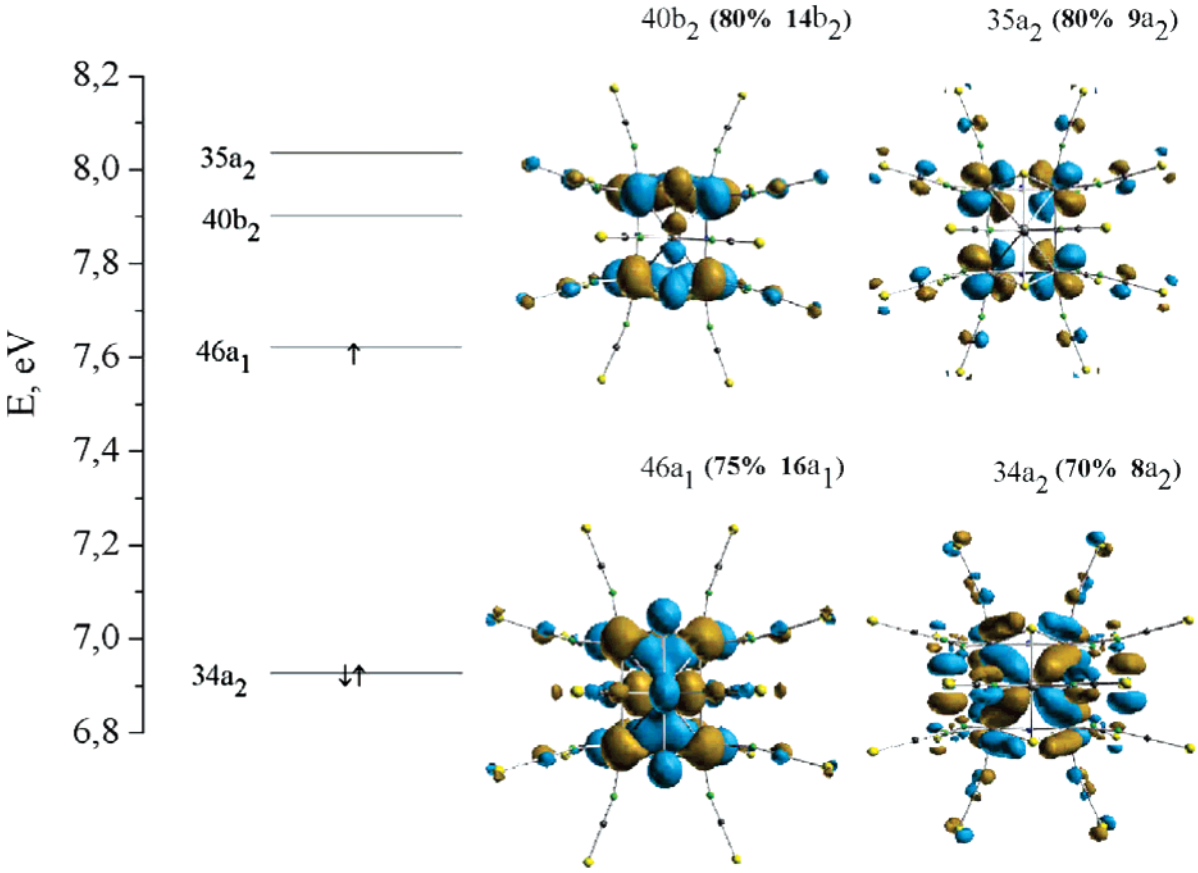

Figure 8. Schematic electronic levels and figures of MOs for C_{2v} $[Nb_5O_4S_2(NSC)_{14}]^{6-}$ Indicated are the numbers and symmetry types of the calculated MOs. Numbers in brackets indicate the percentage of the contributing MO of $Nb_5O_4S_2^{8+}$.

tetramer must possess a structure similar to that of $[Nb_4(\mu_4\text{-}S)(\mu_2\text{-}O)_5(H_2O)_{10}]^{4+}$, with capping O in place of S and bridging OH instead of O.[26]

In the 1:1 equilibration reaction of $Nb_4SO_5^{4+}$ with NCS^-, only a single $[NCS^-]$-dependent reaction is observed, although there are four different types of water present (designated *a*, *b*, *c*, and *d*).

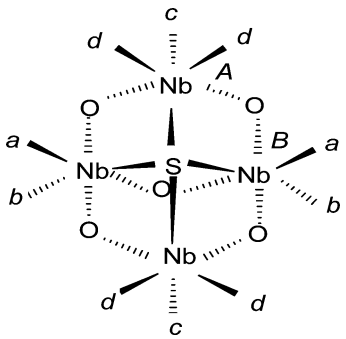

Rate constants with $[NCS^-]$ in excess correspond to those obtained with $[Nb_4SO_5^{4+}]$ in excess only if a statistical factor of 4 is applied, which is surprising because two structurally different types of Nb atoms (designated *A* and *B*) exist. Statistical factors that allow for the simultaneous substitution at more than one equivalent metal site in cluster aqua ions are well-documented. For example, the statistical factor of 4 identified for $[Mo_4S_4(H_2O)_{12}]^{4+}$ ion has been attributed to the four equivalent metal sites in the cluster,[27] whereas factors of 3 and 2 were identified for $[W_3O_4(H_2O)_9]^{4+}$ ion and $[W_2O_4(H_2O)_6]^{2+}$, respectively.[28,29] The present results therefore suggest that the waters on the two different types of Nb do not have substantially different substitution rates, and as such, an averaged rate constant of 9.5 M^{-1} s^{-1} is observed. An alternative explanation is that the four Nb atoms are equivalent in solution despite the solid-state structure.

A comparison of substitution properties between the tetrameric $Nb_4SO_5^{4+}$ and the dimeric $Nb_2(S_2)_2^{4+}$ aqua ions is relevant, as both are d^1 Nb(IV). The $Nb_4SO_5^{4+}$ aqua ion (9.5 M^{-1} s^{-1}) is about 10 times more labile than the $Nb_2(S_2)_2^{4+}$ aqua ion (0.88 M^{-1} s^{-1}).[5] Furthermore, no dependence on $[H^+]^{-1}$ over the range 0.50−2.00 M is observed for $Nb_4SO_5^{4+}$, whereas an enhancement in rate provided by a $[H^+]^{-1}$ term is reported for $Nb_2(S_2)_2^{4+}$. Labilization by the OH^- ligand as a result of H_2O conjugate-base formation, which is indicative of a dissociative mechanism, has been proposed for substitution on the dimeric Nb(IV) aqua ion. However, for $Nb_4SO_5^{4+}$, there is no contribution from the conjugate-

(25) Routledge, C. A.; Sykes, A. G. *J. Chem. Soc., Dalton Trans.* **1992**, 325.
(26) Stünzi, H.; Rotzinger, F. P.; Marty, W. *Inorg. Chem.* **1984**, *23*, 2160.
(27) Li, Y. J.; Nasreldin, M.; Humanes, M.; Sykes, A. G. *Inorg. Chem.* **1992**, *31*, 3011.
(28) Ooi, B. L.; Petrou, A. L.; Sykes, A. G. *Inorg. Chem.* **1988**, *27*, 3626.
(29) Sharp, C.; Hills, E. F.; Sykes, A. G. *J. Chem. Soc., Dalton Trans.* **1987**, 2293.

base form. This can be understood if an associative pathway involving the aqua ion is more favorable, thereby excluding any significant contribution from the conjugate-base form. This is a general feature for metal ions with low d-electron populations, which is the case for Nb(IV), and has been observed with d^1 and d^2 hexa-aqua metal ions such as $[Ti(H_2O)_6]^{3+}$,[30] $[Mo(H_2O)_6]^{3+}$,[31] and $[V(H_2O)_6]^{3+}$.[32] Interestingly, water-exchange reaction on the Nb(III,IV_2) aqua ion, $[Nb_3(Cl)O_3(H_2O)_9]^{4+}$, shows no conjugate-base labilizating effect either, and an associative mechanism has been deduced from activation parameters.[4,33] The π-electron donation from the S_2^{2-} to the Nb(IV) in $Nb_2(S_2)_2^{4+}$, which increases the electron density at the Nb atoms, may be responsible for the anomalous behavior.

The equilibrium constant of 365 M^{-1} for NCS^- substitution on $Nb_4SO_5^{4+}$ indicates a high affinity for thiocyanate. This value is comparable to the 1:1 formation constant for $Nb_2(S_2)_2^{4+}$.

Studies on the 1:1 equilibration of NCS^- with the pentameric Nb(IV) aqua ion, $Nb_5S_2O_4^{8+}$, were limited by the rather small absorbance changes and difficulty in obtaining a high enough concentration in HPTS solution. From the limited data obtained, there are signs of saturation kinetics suggesting that ion-pair formation could be relevant, and a value of 0.2 s^{-1} is estimated for ligand substitution within the ion pair. A large ion-pair formation constant can be expected for NCS^- with such a highly charged positive ion as $Nb_5S_2O_4^{8+}$. Interestingly, the estimated substitution rate in the ion pair is slower than for the rate of substitution on $Nb_4SO_5^{4+}$ but close to the rate of substitution on the conjugate base of $Nb_2(S_2)_2^{4+}$ (0.47 s^{-1}). The $Nb_5S_2O_4^{8+}$ ion possesses two μ_3-S groups, which could be accountable for this trend. Previous studies on the $Mo(IV)_3$ aqua ions $[Mo_3O_{4-x}S_x(H_2O)_9]^{4+}$ have revealed that the μ_3-S ligand has an electron-withdrawing effect and brings about a retardation in substitution rates.[33,34]

This hypothesis of an electron-withdrawing effect of the μ_3-S ligand is supported by the EPR spectroscopic study on $Nb_5S_2O_4^{8+}$. The rather high $\mathbf{g}_y$ value of 2.399 observed suggests that the unpaired electron in $Nb_5S_2O_4^{8+}$ in this axis, which is probably delocalized over all five Nbs in the cluster, is drawn away from the filled inner Nb orbitals. This effect might also arise from interactions with the neighboring Nb atoms in the cluster. However, this is not observed in EPR spectra of the paramagnetic $[(Nb_6Cl_{12})Cl_6]^{3-}$ cluster,[35] where intrinsic isotropy was observed. Contrary to the effect of the μ_3-S ligand, the μ_3-O ligands repel the unpaired electron toward the Nb nuclei, so a significant electron shielding is observed that gives a $\mathbf{g}_z$ value as low as 1.531. This complete lack of symmetry of the cluster so evident in the EPR data is also hinted at in the UV−visible spectrum (Figure 1, right) and the MO diagram in Figure 7, where at least three possible d−d transition bands are observed.

In conclusion, we describe here the synthesis of novel tetranuclear and pentanuclear niobium−sulfido cluster aqua ions in aqueous solution. It is beginning to emerge that niobium has a tendency to form new cluster forms, whereby the familiar triangular $M_3(\mu_3\text{-}X)(\mu_2\text{-}X)_3$ unit is a basic structural motif. This work lends support to the existence of a potentially rich and exciting chemistry for niobium in aqueous solution. Further work is warranted to define the rules and conditions underpinning the chemistry and formation of the unusual clusters seen for niobium.

Acknowledgment. We thank the Institute of Inorganic Chemistry, Russian Academy of Science, Novosibrisk, Russia, for a leave of absence and the Technical University of Denmark for financial support to M.N.S.

Supporting Information Available: X-ray crystallographic data in CIF format. This material is available free of charge via the Internet at http://pubs.acs.org.

IC052145I

(30) Diebler, H. *Z. Phys. Chem.* **1969**, *68*, 64.
(31) Patel, R. C.; Diebler, H. *Ber. Bunsen-Ges. Phys. Chem.* **1972**, *76*, 1035;
(32) Baker, B. R.; Sutin, N.; Welch, T. J. *Inorg. Chem.* **1967**, *6*, 1948.
(33) Richens, D. T. *Chem. Rev.* **2005**, *105*, 1961.
(34) Ooi, B. L.; Martinez, M.; Sykes, A. G. *J. Chem. Soc., Chem. Commun.* **1988**, 1324.
(35) Mackay, R. A.; Schneider, R. F. *Inorg. Chem.* **1967**, *6*, 549.